Reliability Impact of Distributed Energy Resources on Bulk Electric System

N. KANG, R. SINGH, W. KOU
Argonne National Laboratory
USA

N. U. SEGAL
North American Electric Reliability Corporation
USA

J. T. REILLY
Reilly Associates
USA

SUMMARY

High penetration of distributed energy resources (DERs) on modern distribution systems introduces intermittent power generation, stochastic system operating conditions and bi-directional power flows that may affect system responses to various types of disturbances which may pose challenges to the operations and reliability of the Bulk Electric System (BES). This paper describes state-of-the-art modeling and analysis that can help reliability coordinators, planning coordinators and grid operators to understand these impacts and offers solutions to the challenges. The combined modeling of transmission and distribution (T&D) systems on the MATLAB/Simulink platform is an initial step toward identifying the challenges and finding solutions. This platform enables accurate studies of BES steady state and dynamic responses. This paper presents five benchmark case studies which are conducted using the T&D combined model. These benchmark case studies consider DERs' interconnection requirements such as ride-through and islanding and advanced control capabilities that impact the dynamic behavior of DERs. Key findings from BES voltage stability, frequency regulation and dynamic stability analyses show that increasing DER penetration levels tend to degrade BES reliability. Insights on mitigation measures are also offered.

KEYWORDS

Bulk Electric System, distributed energy resource, dynamic stability, frequency regulation, voltage stability, T&D combined model, reliability impact.

kang@anl.gov

I. INTRODUCTION

Stimulated by ambitious state legislation and incentives, and rapid technological progress that drives prices down, industries are increasingly adopting distributed renewable resources (DERs) in their generation portfolio. New York, Oregon, and the District of Columbia expanded their mandates for renewable generation to reach 50% of their total electricity generation by 2030, 2032, and 2040, respectively [1]. The California Energy Commission stipulates that publicly owned utilities procure half of the state's electricity from renewable sources by 2030 [2]. As DERs continue to penetrate the grid, technical problems and reliability challenges emerge, which if not addressed promptly will hinder wide deployment of DERs.

Until recently, challenges and solutions with respect to DER integration into distribution grid were the centerpiece of the research and development effort. DERs' impacts on the Bulk Electric System (BES) were mostly ignored. However, in recent years influences on the BES caused by high DER penetration in the distribution system have become more apparent. First and foremost, the high penetration of DERs on distribution systems introduces intermittent power generation, stochastic system operating conditions and bi-directional power flows that may affect the system responses to various types of disturbances and may pose challenges to the operations and reliability of the BES. Therefore, it is important for regulators, planning coordinators and grid operators to fully understand the reliability impact of high-penetration DERs on the BES and ensure secure and reliable grid planning and operations.

This paper is intended to bring attention to the full-spectrum impact of high-penetration DERs on the BES and modeling and provide analytical approaches to finding solutions to the challenges that these impacts present. Modeling solutions are most often found in planning and operations studies. For BES planning and operations studies, the distribution system typically is represented as a single static load at a transmission node, where generation is netted with load. Modeling a single static load for distribution systems with a high penetration of DERs is insufficient as this model fails to represent the DER dynamic characteristics and the effects of the unbalanced system. To study BES steady state and dynamic responses, aggregating DER models with similar characteristics and/or using reduced-order dynamic equivalent DER models are recommended in current practice [3]. One such example is PVD1, which is an aggregated dynamic equivalencing PV model recommended by WECC [4]. However, the modeling simplicity achieved in this case comes with the price of compromised modeling accuracy. To fill this gap, a combined modeling of transmission and distribution systems (hereafter interchangeably referred to as the T&D combined model) is developed on the MATLAB/Simulink platform. The T&D combined model thoroughly models all of the DERs (single-phase and three-phase) interconnected at the distribution grid, which allows accurate studies of their impacts on bulk system power flows and dynamic performance.

In addition, the emergence of high-penetration DERs requires new considerations in conventional BES steady state and dynamic analyses [5], [6]. For example, the revised BES studies should factor in the impact of interconnection requirements such as ride-through and islanding to represent the dynamic behavior of DERs [7], [8]. The motivation of this paper is to provide a guideline for analyzing the reliability impact on modern BES featured by high DER penetration. Specifically, five benchmark case studies are conducted using the developed T&D combined model in this paper. These benchmark case studies cover DERs' impact on the voltage stability, frequency regulation and dynamic stability of BES considering DER interconnection standards.

The remainder of the paper is organized as follows: Section II introduces the T&D combined model developed on the MATLAB/Simulink platform; Section III describes benchmark case studies using the developed T&D combined model; and Section IV offers conclusions that can be drawn from the modeling and case studies and points to future work to further research in this area.

II. COMBINED MODELING OF TRANSMISSION AND DISTRIBUTION SYSTEMS

The diagram of the T&D combined model developed in MATLAB/Simulink is shown in Fig. 1. The transmission system is the modified Kundur Two-Area network [9]. The two area systems are connected by two 220 km transmission lines modeled with the distributed parameter line model. This model is selected to faithfully represent all the operation modes and dynamics of a BES. The distribution system modeled is the modified IEEE 34-node test system [10] with the inverter-interfaced DER integration. Each DER is interconnected to the distribution system through its point-of-common-coupling (PCC). Distribution systems represented as DS in Fig. 1 below, are connected to the transmission network to replace some of the original load centers. When DER penetration is introduced and increased in an area, the rotational machine-based generation capacity and overall inertia in that respective area are scaled down proportionally to reflect the effect of DER displacing conventional generators.
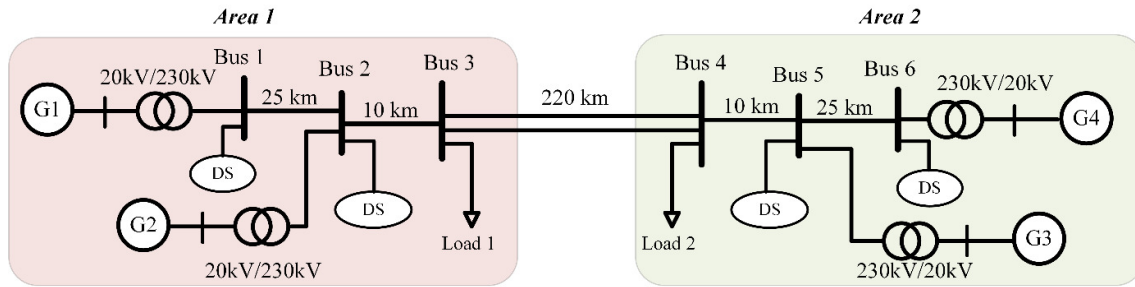

Fig. 1 Diagram of the T&D combined model for benchmark case studies.

The DER model includes a detailed representation of grid-connected DER inverter interface as shown in Fig. 2. The control objective of the DER is to regulate the active and reactive power exchange (P_g, Q_g) between the DC link and the connected distributed grid following the reference value (P_g^*, Q_g^*). The decoupled double synchronous reference frame current controller is adopted for realizing the DER active and reactive power control. Each DER has its own circuit breaker and protection logic scheme which is implemented based on IEEE Std. 1547a-2014 [8]. The time step used for the simulation is 50 µs.
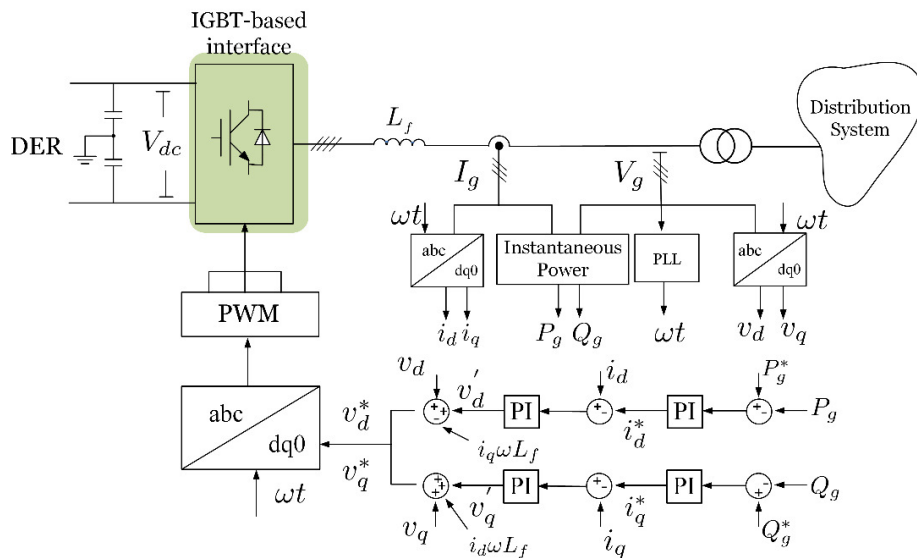

Fig. 2 Schematic diagram of the inverter-interfaced DER model.

III. BENCHMARK CASE STUDIES

A. Voltage Stability

In this case study the continuation power flow is utilized to determine the real power flow and voltage stability margins for the BES under different PV penetration levels. The PVs are integrated in the distribution system connected to Bus 4 in Area 2. The PV penetration level experimented includes 10%, 20%, 30%, 40%, and 50%.

The voltage stability margins corresponding to different PV penetration levels are shown in Fig. 3. This illustrates the relationship between the receiving power (P) and the voltage (V) at Bus 4 in Area 2 known as a P-V curve or nose curve. The x-axis represents system loadability, λ, which is defined as follows [11]:

$$P_L = P_{L,base} + \lambda\left(k_L P_{L,base}\right)$$

where P_L is the varying load condition, $P_{L,base}$ is the base load condition, and k_L is a multiplier to designate the rate of load change as λ changes. λ represents the load parameter such that

$$0 \leq \lambda \leq \lambda_{max}$$

When $\lambda = 0$ corresponds to the base load condition and $\lambda = \lambda_{max}$ corresponds to the maximum or critical load condition. The saddle-node bifurcation point in each P-V curve represents the maximum loading (λ_{max}) of the BES, by which the stability margin could be defined. The voltage stability margin decreases gradually with the PV penetration level increasing from 10% to 50%. It can be noted that the increased PV generation will have a counteractive effect on the BES voltage stability as it will increase the power transfer burden of the transmission lines and then increase the risk of the system voltage collapse.
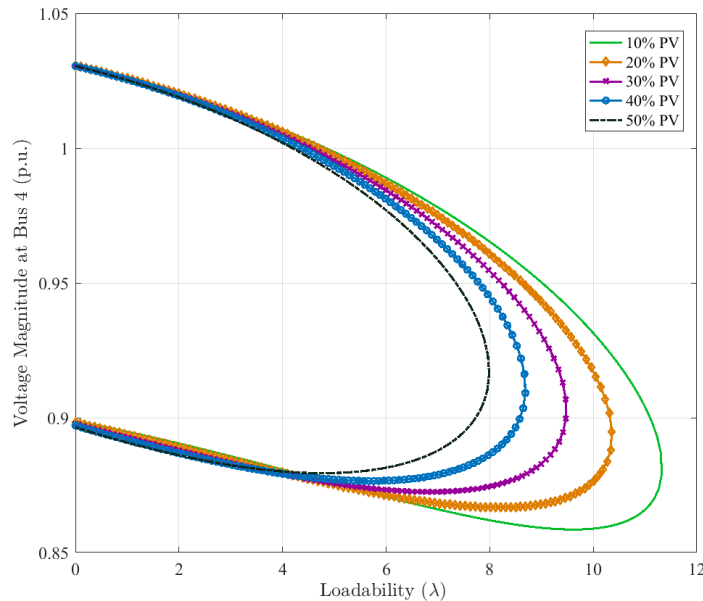

Fig. 3 BES voltage stability margins for different PV penetration levels.

B. Small Signal Stability

To investigate the impact of DER penetration on BES small signal stability, eigenvalue analysis is performed on the linearized model of BES integrated with DERs. In this case study, the DERs are

integrated in Area 2 with 0%, 13% and 30% penetration levels, respectively, as compared to the total load in Area 2. The eigenvalues of the BES for different DER penetration levels are obtained from the system matrices. Fig. 4 shows the eigenvalue plot corresponding to the three levels of DER penetration. In the plot, the direction of pole movement is indicated by the arrows. It is evident from the plot that without DER, the poles of a linear BES all lie in the left half of the s-plane. As the DER penetration level increases, the poles move towards the right half of the s-plane and this indicates the small signal stability of the linear system is degraded.
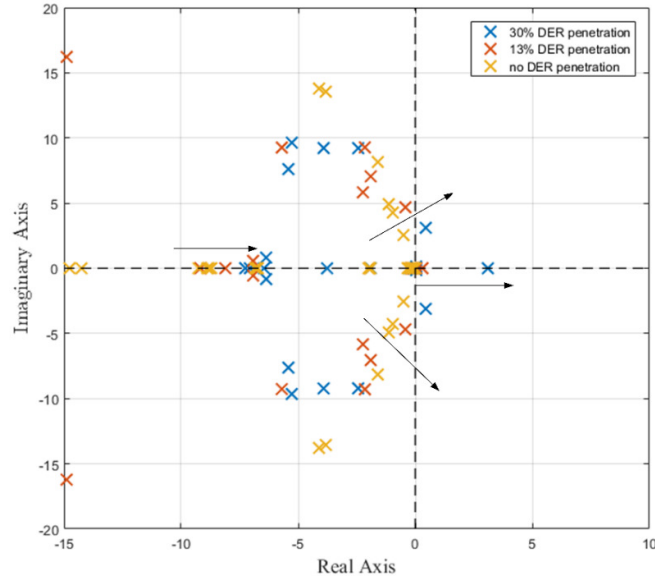

Fig. 4 Pole map of the linear BES with various DER penetration levels.

Table I summarizes the critical eigenvalues in close proximity to the origin for the three different DER penetration levels. The corresponding damping ratios and dominant states contribution to these eigenvalues are also shown in Table I. The results indicate that the main contribution to the eigenvalues for cases with low penetration of DERs, correspond to synchronous machines (G1-G4) in the Two-Area transmission network. When the DER penetration level increases from 13% to 30%, the number of eigenvalues with positive real part is increased from one to four, and the maximum positive magnitude is increased from 0.308 to 3.101. Comparing the damping ratios of 13% DER and 30% DER scenarios, the number of negative damping ratios is increased from one to four, which means the average damping ratio level is weakened. It should also be noted that as the penetration of DER grows, the state controlled by the synchronous machines loses its dominant positions in the entire BES model.

Table I: Critical eigenvalues, damping ratios and dominant states of the linear BES for different DER penetration levels

Eigenvalue Real Part			Damping Ratio			Dominant State		
0% DER	13% DER	30% DER	0% DER	13% DER	30% DER	0% DER	13% DER	30% DER
-0.96	-0.421	0.447	0.219	0.089	-0.142	G2	G2	-
-1.991	-1.929	3.101	1	1	-1	G1	-	-
-0.504	-1.989	-3.763	0.194	1	1	-	G1	-
-0.504	-1.98	-1.984	0.194	1	1	-	G4	G1
-1.912	-1.97	-1.927	1	1	1	G1	G4	-
-1.931	0.308	-1.901	1	-1	1	-	G4	-
-1.991	-0.31	-1.929	1	1	1	-	-	-
-0.319	-0.305	-0.306	1	1	1	G2	-	-
-0.23	-0.307	-0.306	1	1	1	G2	-	-
-0.304	-0.305	-0.31	1	1	1	G2	-	-
-0.314	-0.187	-0.237	1	1	1	G4	-	-

-0.304	-0.171	-0.303	1	1	1	G4	-	-
-0.199	-0.15	0.04	1	1	-0.282	G4	-	-
-0.135	-0.101	0.04	1	1	-0.282	G2	-	-

C. Transient Stability

To study the impact of DERs on the transient stability of BES, two scenarios are created, with DER penetration levels at 15% and 50%. The DERs are integrated in the distribution system connected at Bus 2 in Area 1. It is noteworthy that all the DER systems are designed to operate in PQ mode, where Q is set at 0 throughout the case study. After 1 s into the simulation, a three-phase-to-ground fault with zero impedance is applied at 44 km from Bus 3 on one of the tie-lines from Bus 3 to Bus 4 (in Fig. 1). The fault is cleared in 12 cycles by circuit protection relays, placing the faulted tie-line out of service. The total simulation time is 16 s. The DER response to abnormal frequencies and voltages is implemented according to IEEE Std. 1547a-2014 [8].

The system responses, including tie-line two-terminal (Bus 3 and Bus 4) voltages and active power, DER active and reactive power, for the 15% DER penetration scenario are shown in Fig. 5. DER trigger signal, and frequency and voltage at the DER PCC for the 15% DER penetration scenario are shown in Fig. 6. For the DER trigger signal, value 1 indicates that the DERs stay connected and value 0 indicates that the DERs are tripped off because of either abnormal voltage or abnormal frequency. The transmission-line-fault-induced phenomena for the 15% DER penetration scenario include: a) voltage sags both at the two tie-line terminals and the DER PCC; b) temporary spikes both in the tie-line active power and DER active and reactive power output; and c) temporary frequency excursions measured at the DER PCC. The results show that the voltage and frequency excursions experienced at the DER PCC are not enough to trigger the DERs offline. Fig. 5 and Fig. 6 show that after the fault is cleared by the transmission protection devices, all the quantities return to normal values; system stability is maintained throughout the entire disturbance. The time taken for the BES to recover to a normal state is 4.1 s.
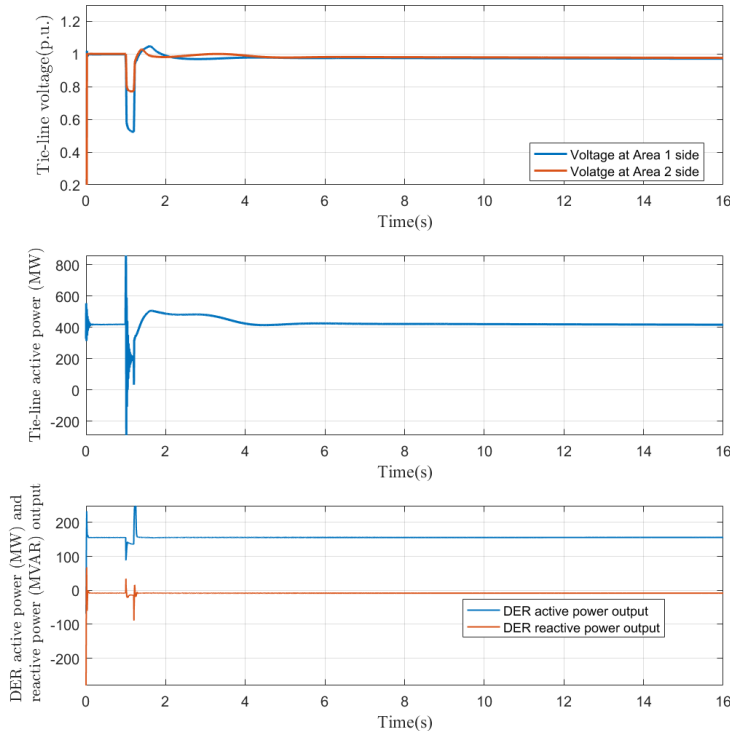

Fig. 5 Tie-line two terminal voltages and active power, and DER active and reactive power for 15% DER penetration scenario.

Fig. 7 and Fig. 8 delineate the system responses for the 50% DER penetration scenario. The results in Fig. 7 and Fig. 8 demonstrate that the transient stability of BES is affected as DER penetration is increased to 50%. In this scenario, the transmission-line-fault-induced phenomena during the fault exhibit similar characteristics to those in the 15% scenario. However, after the fault is cleared, large frequency and voltage deviations at the DER PCC are observed. Eventually the DERs trip offline at 2.01 s as a result of overvoltage protection. Post tripping of the DERs, the system experiences a few cycles of large oscillations as shown in the tie-line two-terminal voltages and active power, before returning to normal conditions.
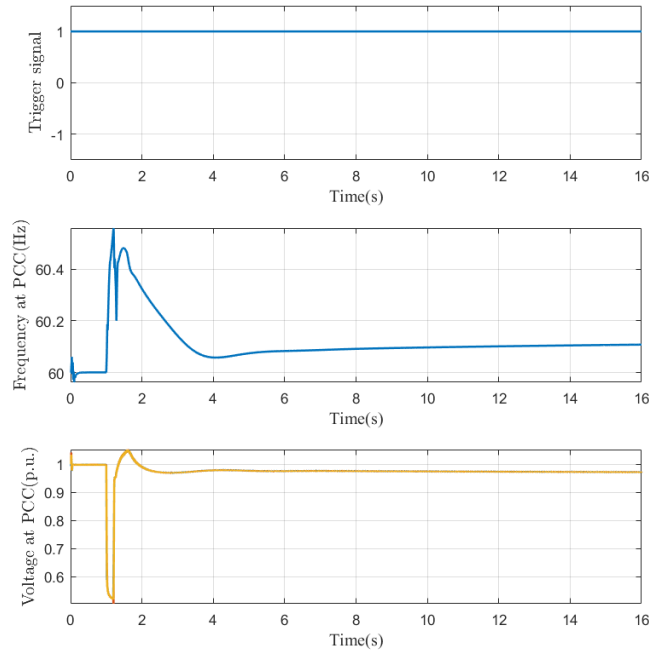

Fig. 6 DER trigger signal, and frequency and voltage at the DER PCC for 15% DER penetration scenario.

Fig. 7 and Fig. 8 show that during the oscillation period, the system shows a tendency toward transient instability. In this scenario, it takes the BES more than 15 s to return to normal state. Thus, it may be inferred that higher DER penetration may put the power grid at risk of instability after a severe transmission system fault. New capabilities of DERs recommended by the IEEE Std. 1547-2018 [12] may contribute to maintain system transient stability. These capabilities include extended voltage and frequency ride-through requirements and providing additional fast reactive power support during fault conditions.
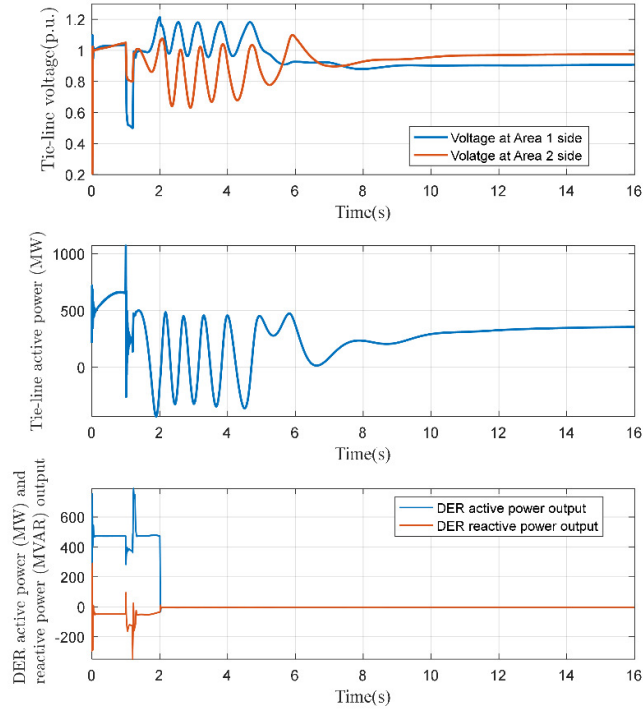
Fig. 7 Tie-line two terminal voltages and active power, and DER active and reactive power for 50% DER penetration scenario.
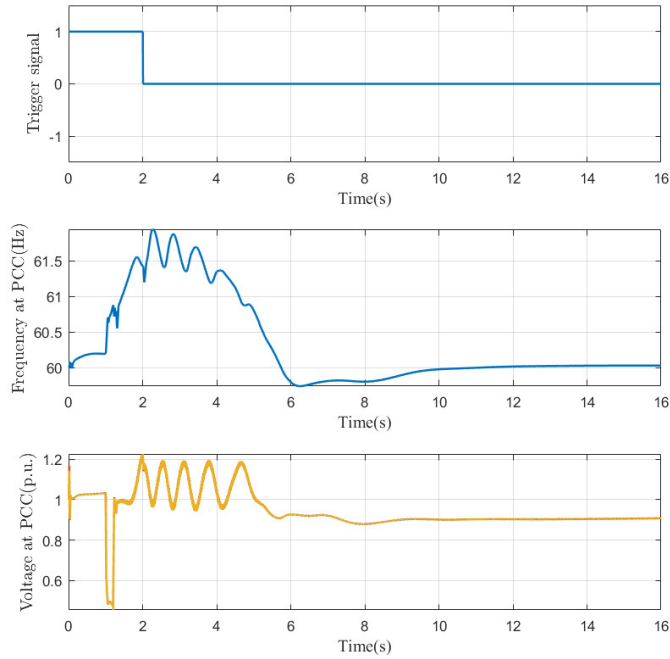

Fig. 8 DER trigger signal, and frequency and voltage at the DER PCC for 50% DER penetration scenario.

D. BES Frequency Regulation

In this case study, the impact of DER on BES frequency regulation is examined. The frequency regulation investigated includes BES inertial response, primary frequency response, and automatic generation control (AGC). The total simulation time is 100 s. A disturbance of an instantaneous load increase in the amount of 160 MW is introduced at 20 s in Area 1. Four sets of simulations are conducted in which the DER penetration level in Area 2 is increased from 0%, 10%, 40%, to 70%

with respect to the total load in Area 2. Fig. 9 provides the deviations from the 60 Hz nominal frequency for all DER penetration scenarios for synchronous generator (SG) #3 in Area 2. For each DER penetration level, the capacity and inertia of all the SGs in Area 2 are reduced proportionally to simulate the effect of DERs displacing SGs and reducing total system inertia. Select frequency response metrics measured at SG #3 are shown in Table II.
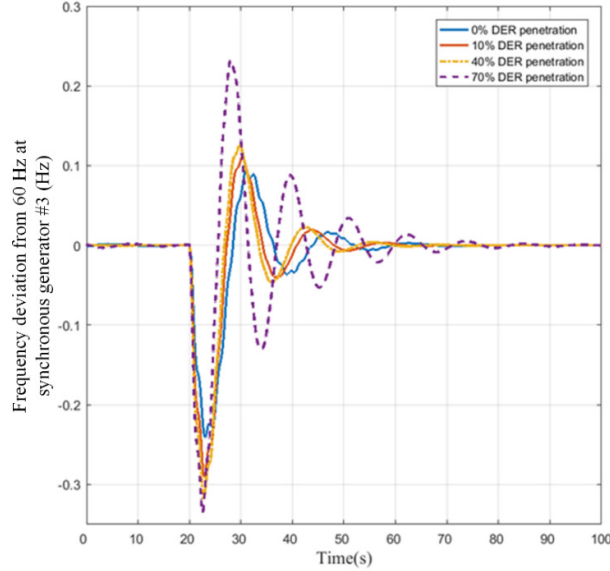

Fig. 9 Impact of different levels of DER penetration on BES frequency regulation.

Frequency Nadir and Initial Rate of Change of Frequency (ROCOF) columns of Table II show the inertial frequency response of the system from different levels of DER penetration. The results indicate that as system inertia is decreased, the initial ROCOF will be higher and the frequency nadir will be lower upon the disturbance. To help maintain system inertial frequency response, virtual synchronous generators (VSGs) may prove to be an effective technology. DERs equipped with advanced control algorithms to emulate the characteristics of synchronous generators are primary examples of VSGs.

Table II: Summary of various frequency response metrics at SG #3

DER Penetration Level	Frequency Nadir (Hz)	Initial ROCOF (Hz/s)	Frequency Oscillation (Hz)	Frequency Settling Time (s)
0%	59.7534	0.0813	0.3356	40
10%	59.7099	0.1018	0.4000	45
40%	59.6824	0.1163	0.4452	55
70%	59.6659	0.1325	0.5646	70

Table II also provides measurements of frequency oscillation and the settling time for all DER penetration scenarios. Frequency oscillation refers to the change in frequency magnitude from the nadir to the first spike during the rebound period. This case study demonstrates that AGC is a critical function to restore system frequency to nominal values after a disturbance. However, when the DER penetration level increases, it is more challenging for AGC to recover system frequency as evidenced by the longer frequency restoration times. Larger and longer frequency oscillations during the disturbance are observed for higher DER penetration scenarios. The system's inability to quickly dampen these large swings could cause more equipment to trip off in order to protect itself, possibly leading to a cascading failure.

E. BES Net Load Variability and Ramping

In this case study, Bus 2 in Area 1 in the Kundur Two-Area system (shown in Fig. 1) is modeled as the swing bus. The remaining transmission system buses are modelled as PQ buses. The load connected to Bus 4 is replaced with a distribution system integrated with PVs. The following levels of PV penetration 10%, 20%, 30%, 40%, and 50% are investigated at Bus 4. The 24-hour load and PV profile data are collected from the California ISO (CAISO) 2017 real-time operational data [13] and both are scaled down by the order of magnitude of ten to align with the case's transmission network load rating.

The 24-hour BES net load profile in terms of active power is shown in Fig. 10 for all five levels of PV penetration (applied at Bus 4). Net load of a BES is defined as the actual total load minus the generation from variable generation resources such as wind and PV. The variable generation resources in this case study refer to PVs connected at the distribution system. The BES net load shown in the figure exhibits a duck curve characteristic similar to that produced by CAISO. Fig. 10 demonstrates that PV integration causes the system net load to drop during the day due to the power supply from the PVs and then to ramp up at a faster rate during the evening hours as the sunset coincides with a period of increased load demand. The three-hour BES ramping from 5pm to 8pm increases from 717 MW to 1424 MW (i.e., approximately twice the initial value) as the PV penetration is increased from 10% to 50%. Therefore, without PV curtailment or enacting other mitigating methods, it is evident that as the PV penetration level increases, the challenges for BES net load variability and ramping will also increase. PV curtailment and load management schemes such as shifting some load consumption from evening hours to daytime hours are potential measures to flatten the duck curve. Moreover, dispatchable resources such as electric vehicles (EVs) and battery energy storage systems (BESS) can be integrated to the grid to help relieve the net load variability and ramping challenges. EVs and BESS can be charged during the day when there is a PV surplus and discharge in the evening when PVs drop out and load increases.
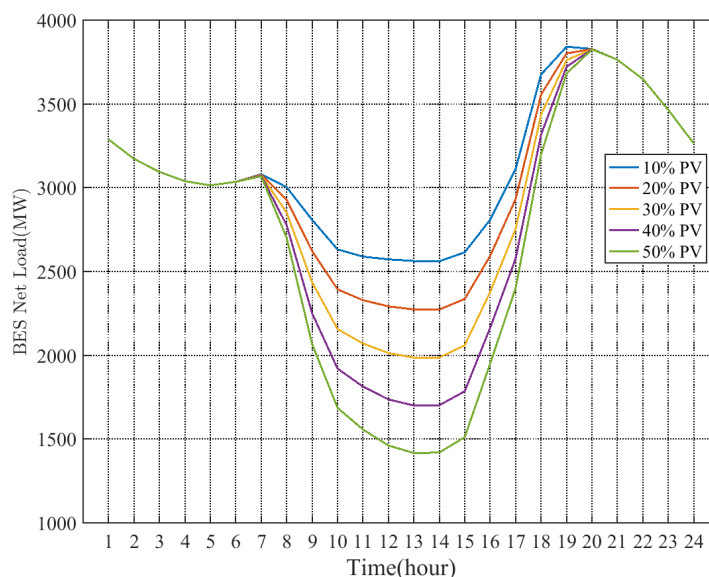

Fig. 10 Impact of DER on BES net load variability and ramping.

IV. CONCLUSION

In this paper, a T&D combined model in MATLAB/Simulink environment is shown to be an improvement over existing distribution system modeling techniques insofar as it allows reliability organizations, planning coordinators, and grid operators to understand the reliability impact imposed on the BES due to high-penetration of DERs that are connected to the distribution system. A total of five benchmark case studies are investigated using the T&D combined model. Results from these studies show the DERs' impact on BES voltage stability, small signal stability, transient stability, BES frequency regulation, and BES net load variability and ramping. The findings of these case studies are:

1. Voltage stability – higher PV generation tends to increase the power transfer burden on transmission lines which in turn increases the risk of the system voltage collapse.
2. Small signal stability – small-signal stability analysis of the BES shows that the eigenvalues tend to move to the right half of the s-plane as the level of DER penetration increases; hence, making the system more susceptible to instability caused by small disturbances.
3. Transient stability – higher DER penetration conditions may lead to oscillations, DERs tripping offline, and a longer time for the system to return to normal operating conditions. Furthermore, if mitigating methods are not enacted then with increasing levels of DER penetration, there is an increased risk to instability after a severe transmission system fault.
4. BES frequency regulation – overall bulk system inertia is reduced as the number of DERs replacing SGs increases, which given a disturbance results in higher initial ROCOF and a lower frequency nadir; additionally, larger and longer frequency oscillations associated with higher DER penetration scenarios are observed which indicate an increased risk to the possibility of cascading failures.
5. BES net load variability and ramping – high DER penetration creates high net load variability and ramping challenges for the BES, with plots exhibiting similar characteristics to duck curves produced by CAISO.

Future work on the mitigation of adverse reliability impacts of high-penetration DERs on the BES should be directed towards using advanced control capabilities for the management of DERs, such as high-speed energy injections, emulated inertia through VSG technologies, dynamic VAR support, and droop control for frequency regulation. Employing advanced control capabilities would transform DERs from a passive "do no harm" resource to an active "support reliability" resource. In addition, power system protection studies are needed to investigate the impact of high DER penetration on coordination among distribution-system protection devices and DER protection devices, other protection schemes such as undervoltage load shedding and under frequency load shedding schemes. The results of the protection studies should be used to determine: (a) appropriate DER frequency and voltage ride-through settings; and (b) distribution system protection devices settings. These studies will help ensure bulk system reliability and also satisfy distribution-system safety requirements (e.g., prevention of unintentional utility islanding).

ACKNOWLEDGEMENT

BIBLIOGRAPHY

[1] C. Marcy, "Renewable generation capacity expected to account for most 2016 capacity additions," https://www.eia.gov/todayinenergy/detail.php? id=29492, accessed January 2017.

[2] "California renewable energy overview and programs," http://www.energy.ca.gov/renewables/.

[3] NERC, "Distributed energy resources connection modeling and reliability considerations," February 2017.

[4] WECC Renewable Energy Modeling Task Force, "WECC solar power plant dynamic modeling guidelines," April 2014.

[5] J. Liu, W. Zhang, R. Zhou, and J. Zhong, "Impacts of distributed renewable energy generations on smart grid operation and dispatch," in *Proc. 2012 IEEE Power and Energy Soc. General Meeting*, 2012, pp. 15.

[6] Y. Zhang, A. Allen, and B. M. Hodge, "Impact of distribution-connected large-scale wind turbines on transmission system stability during large disturbances," in *Proc. 2014 IEEE Power and Energy Soc. General Meeting*, National Harbor, MD, USA, July 2014, pp. 15.

[7] IEEE, "IEEE Standard for Interconnecting Distributed Resources with Electric Power Systems," IEEE Std. 1547-2003, July 2003, pp. 1–28.

[8] IEEE, "IEEE Standard for Interconnecting Distributed Resources with Electric Power Systems," IEEE Std. 1547a-2014, May 2014.

[9] P. Kundur, N. J. Balu, and M. G. Lauby, "Power system stability and control," McGraw-hill New York, 1994, vol. 7.

[10] "IEEE 34 node test feeder," http://ewh.ieee.org/soc/pes/dsacom/testfeeders/index.html, accessed June 2017.

[11] V. Ajjarapu and C. Christy, "The continuation power flow: a tool for steady state voltage stability analysis," *IEEE Transactions on Power Systems*, vol. 7, no. 1, February 1992, pp. 416–423.

[12] IEEE, http://standards.ieee.org/findstds/standard/1547-2018.html.

[13] "California ISO daily renewables watch," http://www.caiso.com/market/Pages/ReportsBulletins/DailyRenewablesWatch.aspx#curtailment.